

# Partitioning of Alkane and Alcohol Solutes between Water and (Dry or Wet) 1-Octanol

Bin Chen and J. Ilja Siepmann\*

Contribution from the Departments of Chemistry and of Chemical Engineering and Materials Science, University of Minnesota, 207 Pleasant Street SE, Minneapolis, Minnesota 55455-0431

Received March 30, 2000

**Abstract:** Configurational-bias Monte Carlo simulations in the Gibbs ensemble using the OPLS (optimized potentials for liquid simulations) force field were performed to study the partitioning of normal alkane and primary alcohol solutes between water, neat or water-saturated 1-octanol, and helium vapor phases. Precise values of the Gibbs free energy of transfer were calculated directly from the ratio of the solute number densities in the two co-existing phases. It is observed that the OPLS force field yields Gibbs free energies of transfer that are in qualitative, albeit not quantitative, agreement with experimental results. Comparison of the partitioning between a helium vapor and dry or wet 1-octanol phases established that water saturation affects mostly the partitioning of polar solutes, while differences for alkane partitioning were found to be negligible. In addition, the analysis of radial distribution functions of alcohol solutes in wet 1-octanol shows preferential partitioning into water-rich regions of the microheterogeneous solvent mixture.

## Introduction

Knowledge of the 1-octanol/water partition coefficient,  $K_{OW}$ , and the corresponding Gibbs free energy of transfer,  $\Delta G_{OW} = -RT \ln K_{OW}$ , for a given solute are the main ingredients of quantitative structure–activity relationships<sup>1</sup> and have been used to correlate or predict a plethora of solute properties<sup>2</sup> including the pharmacokinetic characteristics of drug compounds in biophases (membranes, adipose tissue, and body fluids)<sup>1,3</sup> and the toxicity and transport of pollutants in soil/groundwater systems.<sup>4</sup> The reasoning behind this is that the partitioning of a solute molecule (drug or pollutant) between a polar aqueous environment and a nonpolar organic environment (e.g., biological membrane or soil) is most often the rate-determining step in biological, environmental, and geological processes. 1-Octanol consists of a hydrophilic head and a lipophilic tail leading to a microheterogeneous solvent phase<sup>5,6</sup> which has been found to mimic particularly well the complexities of biological and other environments. Sangster<sup>2</sup> estimated that experimental  $K_{OW}$  are now available for more than 18 000 solutes, but this number is nowhere close to the number of possible drug molecules (that can be synthesized by combinatorial chemistry approaches) or possible pollutants. In addition, little is known about the effect of water on the solvent characteristics of wet 1-octanol, and the magnitude of the (fictitious)  $\Delta G$  of a solute between dry

and water-saturated 1-octanol has been controversial among different experimental studies.<sup>7–9</sup>

## Simulation Methods

Configurational-bias Monte Carlo (CBMC)<sup>10</sup> simulations in the Gibbs ensemble<sup>11</sup> were carried out to explore the 1-octanol/water partitioning of *n*-alkanes (methane to *n*-butane) and of 1-alkanols (methanol to 1-butanol). The Gibbs ensemble Monte Carlo (GEMC) method is ideally suited for this endeavor because it allows a setup analogous to the experimental situation. GEMC utilizes two (or more) separate simulation boxes which are in thermodynamic contact, but do not have an explicit interface. As a result, for a given state point the properties of the coexisting phases, such as the mutual solubilities of the two solvents and the partitioning of (a few different) solute molecules, can be determined directly from a single simulation. In the GEMC simulations described here (see Figure 1), six different types of Monte Carlo moves are employed to sample phase space efficiently: translational, rotational, CBMC conformational, CBMC swap, CBMC switch, and volume moves. The first three types of moves involve only a single molecule in a given box and ensure thermal equilibration. The CBMC swap move<sup>12</sup> involves the particle exchange of a (solute or solvent) molecule from one phase to the other, thereby equalizing the chemical potentials of each species in the two phases. During a CBMC switch move,<sup>13</sup> molecule A (say, the monomeric square in Figure 1) is regrown as

(7) Schantz, M. M.; Matire, D. E. *J. Chromatogr.* **1987**, *391*, 35–51.

(8) Dallas, A. J.; Carr, P. E. *J. Chem. Soc., Perkin. Trans.* **1992**, *2*, 2155–2161.

(9) (a) Berti, P.; Cabani, S.; Conti, G.; Mollica, V. *Thermochim. Acta* **1987**, *122*, 1–8. (b) Bernazzani, L.; Cabani, S.; Conti, G.; Mollica, V. *J. Chem. Soc., Faraday Trans.* **1995**, *91*, 649–655.

(10) (a) Siepmann, J. I.; Frenkel, D. *Mol. Phys.* **1992**, *75*, 59–70. (b) Frenkel, D.; Mooij, G. C. A. M.; Smit, B. *J. Phys.: Condens. Matter* **1992**, *4*, 3053–3076. (c) Martin, M. G.; Siepmann, J. I. *J. Phys. Chem.* **1999**, *103*, 4508–4517.

(11) (a) Panagiotopoulos, A. Z. *Mol. Phys.* **1987**, *61*, 813–826. (b) Panagiotopoulos, A. Z.; Quirke, N.; Stapleton, M.; Tildesley, D. *J. Mol. Phys.* **1988**, *63*, 527–545.

(12) Mooij, G. C. A. M.; Frenkel, D.; Smit, B. *J. Phys.: Condens. Matter* **1992**, *4*, L255–259.

(13) (a) Martin, M. G.; Siepmann, J. I. *J. Am. Chem. Soc.* **1997**, *119*, 8921–8924. (b) Siepmann, J. I.; McDonald, I. R. *Mol. Phys.* **1992**, *75*, 255–259.

\* Corresponding author. E-mail: siepmann@chem.umn.edu.

(1) (a) Hansch, C.; Fujita, T. *J. Am. Chem. Soc.* **1964**, *86*, 1616–1626. (b) Kamlet, M. J.; Abraham, M. H.; Doherty, R. M.; Taft, R. W. *ibid.* **1984**, *106*, 464–466. (c) Hansch, C.; Leo, A. *QSAR: Fundamentals and Applications in Chemistry and Biology*; American Chemical Society: Washington, DC, 1995.

(2) Sangster J. *Octanol-Water Partition Coefficients: Fundamentals and Physical Chemistry*; John Wiley & Sons: Chichester, 1997.

(3) Connell, D. W. *Bioaccumulation of Xenobiotic Compounds*; CRC Press: Boca Raton, 1990.

(4) (a) Briggs, G. G. *J. Agric. Food Chem.* **1981**, *29*, 1050–1059. (b) Dobbs, R. A.; Wang, L.; Govind, R. *Environ. Sci. Technol.* **1989**, *23*, 1092–1097.

(5) Marcus, Y. *J. Solution Chem.* **1990**, *19*, 507–517.

(6) Debolt, S. E.; Kollman, P. A. *J. Am. Chem. Soc.* **1995**, *117*, 5316–5340.

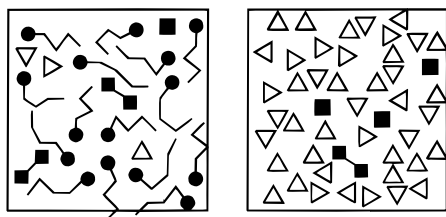


**Figure 1.** Schematic drawing of the Gibbs ensemble setup used to study the partitioning of two solutes (filled monomeric squares and filled dimeric squares) between a water-saturated 1-octanol phase (filled circles with tail segments) and a water phase (open triangles).

molecule B (say, the dimeric square) in one box, and B is regrown as A in the other box. This move has a much higher acceptance rate than the straightforward CBMC swap move of the larger B molecule and is used to equalize the differences in chemical potentials of A and B in the two boxes. Finally, volume moves involving an external pressure bath lead to mechanical equilibrium between the two phases. The main advantages of CBMC/GEMC simulations over the more traditional thermodynamic integration (TI) or free-energy perturbation (FEP) methods<sup>14</sup> are the following: First, in both the experiment and the CBMC/GEMC simulations the Gibbs free energy of transfer is directly determined from the ratio of solute number densities in the two phases (the partition constant),<sup>15</sup> while the difference in excess chemical potentials (related to a specific standard state) is used in TI and FEP calculations. Second, the number density ratio is a mechanical property that can be determined very precisely from CBMC/GEMC simulations leading to small statistical errors in  $\Delta G$ .<sup>15</sup> Third, the composition of the two solvent phases does not need to be specified in advance in CBMC/GEMC simulations, because the distribution of solvent molecules is also sampled via swap moves. Whereas TI and FEP calculations can only be carried out at a fixed composition (e.g., using the experimental data to construct a water-saturated 1-octanol phase), that might not correspond to a proper thermodynamic state for the force field used in the calculations.

The popular TIP4P and OPLS united-atom force fields were used here to describe the interactions of water and the alkanes and alcohols, respectively.<sup>16,17</sup> Spherical potential truncations at 14 Å and analytical tail corrections (for the energy, pressure, and chemical potential) were used for the Lennard-Jones interactions. In addition, an Ewald sum with tin-foil boundary conditions ( $\kappa \times L = 5$  and  $K_{\max} = 5$ ) was used to treat the long-range electrostatic interactions. Simulations in the isobaric version of the Gibbs ensemble ( $T = 298$  K and  $p = 101.3$  kPa) were carried out for four different two-phase systems (see Table 1): G/O, helium/(dry) 1-octanol; G/O\*, helium/(water-saturated) 1-octanol; G/W, helium/water; and W/O, (mutually saturated) water/1-octanol. Because of the low vapor pressures of 1-octanol (0.014 Pa) and water (3.17 kPa), the concentrations of these molecules in the helium vapor phase would be very low. Therefore, swap moves for these molecules were not considered for the G/O and G/W systems. The simulations for the G/O\* case required a fixed composition (determined from a short pre-simulation for the W/O system), and the solvent molecules were thus confined to remain in the liquid phase. Finally, 1-octanol swaps were also not considered in the W/O simulations because of its very low mutual solubility in water ( $7 \times 10^{-5}$  mole fraction). For each of the four systems, five independent simulations of either  $10^5$  or  $2 \times 10^5$  Monte Carlo cycles (production period, one Monte Carlo cycle consists of  $N$  moves where  $N$  is the total number of molecules in the system) were carried out. The resulting

**Table 1.** Numbers of Molecules Used for the Four Systems

molecule type	G/O	G/W	W/O	G/O*
helium	600	600	0	600
methane	20	20	0	20
ethane	20	20	0	20
propane	1	1	0	1
<i>n</i> -butane	1	1	0	1
methanol	1	1	1	1
ethanol	1	1	1	1
1-propanol	1	1	1	1
1-butanol	1	1	1	1
water	0	864 <sup>a</sup>	864	24 <sup>a</sup>
1-octanol	240 <sup>a</sup>	0	240 <sup>a</sup>	240 <sup>a</sup>

<sup>a</sup> Not allowed to swap between phases.

statistical errors in  $\Delta G$  lie between less than 0.1 kJ/mol for methane partitioning between helium and (dry or wet) 1-octanol and about 1 kJ/mol for 1-butanol in the W/O system.

## Results and Discussion

The calculated  $\Delta G$  values are summarized in Table 2. For most of the solutes (except methane, propane, and methanol) the calculated  $\Delta G_{G \rightarrow O}$  were found to be larger in magnitude than their experimental counterparts (with a mean unsigned deviation for all eight solutes of about 1.3 kJ/mol). In particular, the longer the alkane (or alcohol), the larger the deviation. This feature is related to shortcomings in the OPLS description of pure alkane and alcohol phases, where increases in chain length (addition of methylene segments) lead to larger deviations in critical temperatures and heats of vaporization.<sup>18</sup>

For all eight solutes, the calculated  $\Delta G_{G \rightarrow W}$  were found to be higher than the experimental values (with a mean deviation of 1.4 kJ/mol). It is important to note here, that the CBMC/GEMC simulations can easily distinguish between adjacent *n*-alkanes and that the OPLS force field correctly reproduces the minimum in  $\Delta G_{G \rightarrow W}$  for ethane among the *n*-alkanes. Compared to G $\rightarrow$ O partitioning, the G $\rightarrow$ W partitioning shows quite different behavior as function of chain length. The methylene increment in the latter case is much smaller and positive. In addition, the differences in  $\Delta G$  between an alkane and the alcohol with the same number of carbon units (e.g., methane and methanol) is about 10 kJ/mol larger for the transfer to water than to 1-octanol. Again, these qualitative features are well-reproduced by the OPLS force field.

Using a thermodynamic cycle, the  $\Delta G$  between water and neat 1-octanol could now be calculated from  $\Delta G_{G \rightarrow W}$  and  $\Delta G_{G \rightarrow O}$ . However, the experimental setup used to measure  $K_{OW}$  and  $\Delta G_{W \rightarrow O}$  involves mutually saturated 1-octanol and water phases. Thus, in system W/O the water molecules were allowed to equilibrate between the two liquid phases to achieve a water-saturated 1-octanol phase. (There is general agreement that the properties of the water phase are not altered by the very small 1-octanol concentration.<sup>2,7,8</sup>) The resulting TIP4P water mole fraction in OPLS 1-octanol is about 0.09, that is only a third of the commonly accepted experimental concentration.<sup>2,8</sup> Correspondingly,  $\Delta G_{W \rightarrow O}$  for water deviates by +3.6 kJ/mol from experiment. This low mutual solubility for the model system might serve as a warning for FEP and TI calculations because a 1-octanol phase with the experimental water concentration would constitute a thermodynamically unstable state for the TIP4P/OPLS force field. The calculated  $\Delta G_{W \rightarrow O}$  for the four primary alcohol solutes are significantly too low with an average deviation of more than 4 kJ/mol. From a comparison of  $\Delta G_{W \rightarrow O}$

(14) (a) Jorgensen, W. L. *Acc. Chem. Res.* **1989**, *22*, 184–189. (b) Kollman, P. A. *Chem. Rev.* **1993**, *93*, 2395–2417.

(15) (a) Martin, M. G.; Siepmann, J. I. *Theor. Chem. Acc.* **1998**, *99*, 347–350. (b) Martin, M. G.; Siepmann, J. I.; Schure, M. R. *J. Phys. Chem.* **1999**, *103*, 11191–11195.

(16) Jorgensen, W. L.; Chandrasekhar, J.; Madura, J. D.; Impey, R. W.; Klein, M. L. *J. Chem. Phys.* **1983**, *79*, 926–935.

(17) (a) Jorgensen, W. L.; Madura, J. D.; Swenson, C. J. *J. Am. Chem. Soc.* **1984**, *106*, 6638–6646. (b) Jorgensen, W. L. *J. Phys. Chem.* **1986**, *90*, 1276–1284. (c) Jorgensen, W. L.; Tirado-Rives, J. *J. Am. Chem. Soc.* **1988**, *110*, 1657–1666.

(18) (a) Martin, M. G.; Siepmann, J. I. *J. Phys. Chem. B* **1998**, *102*, 2569–2577. (b) Chen, B.; Siepmann, J. I. *ibid.* **1999**, *103*, 5370–5379.

**Table 2.** Gibbs Free Energies of Transfer (in kJ/mol) at  $T = 298$  K and  $p = 101.3$  kPa<sup>a</sup>

solute	simulation				experiment <sup>2,8,20</sup>			
	G→O	G→O*	G→W	W→O	G→O	G→O*	G→W	W→O
methane	+2.68 <sub>4</sub>	+2.81 <sub>8</sub>	+9.4 <sub>2</sub>		+2.14		+8.37	-6.22
ethane	-2.74 <sub>7</sub>	-2.56 <sub>9</sub>	+8.2 <sub>4</sub>		-2.68		+7.66	-10.33
propane	-4.64 <sub>15</sub>	-4.50 <sub>13</sub>	+9.7 <sub>5</sub>		-5.27		+8.20	-13.47
<i>n</i> -butane	-8.7 <sub>3</sub>	-8.8 <sub>3</sub>	+10.7 <sub>7</sub>		-7.78		+8.70	-16.49
water				+11.3 <sub>4</sub>				+7.71
methanol	-15.8 <sub>6</sub>	-17.3 <sub>3</sub>	-19.3 <sub>2</sub>	+2.4 <sub>3</sub>	-16.17	-17.14	-21.19	+4.05
ethanol	-20.2 <sub>5</sub>	-21.1 <sub>3</sub>	-19.5 <sub>4</sub>	-1.6 <sub>6</sub>	-18.22	-19.15	-20.95	+1.80
1-propanol	-22.8 <sub>5</sub>	-23.4 <sub>5</sub>	-18.8 <sub>4</sub>	-5.4 <sub>8</sub>	-20.98	-21.81	-20.36	-1.45
1-butanol	-27.6 <sub>7</sub>	-27.6 <sub>5</sub>	-18.3 <sub>4</sub>	-10.4 <sub>13</sub>	-23.88	-24.64	-19.86	-4.78

<sup>a</sup> The subscripts denote the error of the mean of five independent simulation results.

and  $\Delta G_{G \rightarrow O} - \Delta G_{G \rightarrow W}$  for the alcohol solutes, it is evident that the partitioning between the mutually saturated phases results in a lowering of  $\Delta G$  by about 1 kJ/mol. Thus, consonant with chemical intuition, it is observed that the dissolved water increases the solubility of these alcohol solutes in the 1-octanol phase.

To further study the effect of dissolved water on solubilities in the water-saturated 1-octanol phase, an additional set of simulations was carried out to directly sample the vapor/(water-saturated) 1-octanol partitioning using a 1-octanol phase with a fixed amount of water present (system G/O\*, see Table 1). The  $\Delta G_{G \rightarrow O^*}$  values agree well with those obtained using a thermodynamic cycle of  $\Delta G_{G \rightarrow W} + \Delta G_{W \rightarrow O}$ , but the former has a better statistical accuracy. Comparing  $\Delta G_{G \rightarrow O}$  and  $\Delta G_{G \rightarrow O^*}$ , we observe that the transfer from neat 1-octanol to water-saturated 1-octanol ( $\Delta G_{O \rightarrow O^*}$ ) is favorable for the polar alcohols with methanol showing the most negative  $\Delta G_{O \rightarrow O^*} = 1.5$  kJ/mol and 1-butanol showing no significant preference for either phase. In contrast, the *n*-alkane solutes exhibit positive  $\Delta G_{O \rightarrow O^*}$  of about 0.15 kJ/mol for methane, ethane, and propane; thus, these solutes have a preference for the neat 1-octanol phase. These results are consistent with the experimental data of Dallas and Carr<sup>8</sup> who reported  $\Delta G_{O \rightarrow O^*}$  values from -0.97 to -0.76 kJ/mol for methanol to 1-butanol, respectively, and a value of +0.25 kJ/mol for *n*-nonane. Values of similar magnitude for *n*-alkanes and 1-butanol were determined by Schantz and Matire.<sup>7</sup> However, it should be pointed out that Bernazzani et al.<sup>9b</sup> measured much larger values of -1.76 kJ/mol for 1-butanol and from 2.0 to 1.3 kJ/mol for *n*-hexane to *n*-octane.

One of the prime purposes of molecular simulations for these complex chemical systems is to provide microscopic-level insight on the solvation mechanism.<sup>6</sup> Visual inspections of configuration files for systems W/O and G/O\* show a micro-heterogeneous structure of the water-saturated 1-octanol phase with large hydrogen-bonded water-1-octanol clusters in good agreement with the results of molecular dynamics simulations.<sup>6</sup> The coordination number (up to a distance of 3.5 Å) of water in water-saturated 1-octanol is 3.3 (significantly less than in neat water) with a local mole fraction<sup>5</sup>  $x_{W(W)}^L = 0.15$ , that is significantly higher than the overall mole fraction of  $x_W = 0.09$ . In contrast to thermodynamic arguments,<sup>5</sup> we also observed a local enhancement of the water concentration around 1-octanol molecules with  $x_{W(O)}^L = 0.13$  and a coordination number of about 2.1. This latter number is comparable to the coordination for neat 1-octanol of 2.0, and again agrees with the molecular dynamics calculations,<sup>6</sup> but differs from the theoretical estimate of 1.5.<sup>5</sup> To analyze the effect of water saturation on solubilities, the methanol solute oxygen-solvent oxygen radial distribution functions for systems G/O and G/O\* were calculated (see Figure 2). The large first peaks demonstrates that a methanol solute strongly prefers to solvate in the polar regions of neat and water-

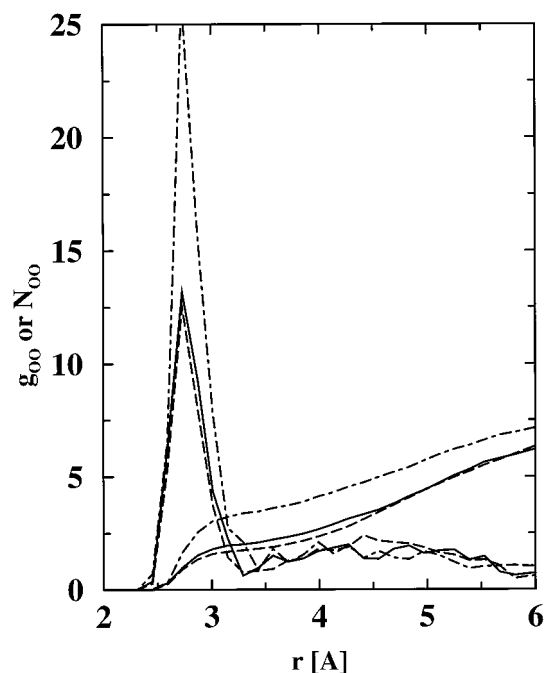


**Figure 2.** Oxygen-oxygen radial distribution functions and their corresponding number densities. Solid, dashed, and dotted lines are used for  $O_{\text{methanol}}-O_{\text{neat octanol}}$  (system G/O),  $O_{\text{methanol}}-O_{\text{wet octanol}}$  (system G/O\*), and  $O_{\text{methanol}}-O_{\text{water}}$  (system G/O\*, number integral scaled by a factor of 10), respectively.

saturated 1-octanol. It is interesting to note that the peak height and the number of neighboring 1-octanol molecules are very similar for neat and water-saturated octanol, but the first peak involving water is almost twice as high, and the local water concentration of methanol is  $x_{W(M)}^L = 0.16$  with an overall coordination number of about 2.2. Actually, the average numbers of hydrogen bonds for 1-butanol solutes are comparable (2.1 and 2.2 for neat and water-saturated 1-octanol, respectively), but the numbers of solvent oxygen atoms within 7 Å are 5% (neat 1-octanol) and 14% (water-saturated 1-octanol) smaller than for methanol. Thus, 1-butanol is found on the boundary of hydrogen-bonded clusters, while methanol is more often embedded in them, which might explain why  $\Delta G_{O \rightarrow O^*}$  is negligible for 1-butanol. In contrast, the nonpolar alkanes preferentially partition into the nonpolar regions of the 1-octanol phase. The coordination numbers (up to a distance of 4.5 Å) for a methane solute in neat (and water-saturated) 1-octanol are 1.9 (2.2) for  $\text{CH}_3$ , 7.7 (8.6) for  $\text{CH}_2$ , and 0.7 (0.8) for all O. Therefore, addition of water expels methane from larger regions of the water-saturated 1-octanol phase, yielding positive  $\Delta G_{O \rightarrow O^*}$  values, albeit this effect is small because of the very low volume fraction of water in this phase.

## Conclusions

The combination of GEMC and CBMC methods allows for the precise determination of Gibbs free energies of transfer of multiple solutes between two phases in which the mutual solubilities of the different solvents play an important role. In particular, the composition of the two solvent phases does not need to be specified in advance but is sampled on-the-fly via swap moves of solvent molecules between the two phases. Thus, the simulation methodology offers significant advantages over more traditional free-energy methods.

Comparison of the Gibbs free energies of transfer between a helium vapor and dry or wet 1-octanol phases demonstrates that water saturation affects mostly the partitioning of small, polar molecules, while differences in the partitioning of nonpolar solutes are negligible. For example, methanol shows preferential partitioning into the water-rich regions of the water-saturated 1-octanol phase, whereas addition of water expels methane from larger regions of the microheterogeneous solvent mixture. Since 1-octanol/water partitioning coefficients have been found to be a better predictor of biological activity than the corresponding hydrocarbon/water partition coefficients,<sup>2,19</sup> we might infer that preferential solubilization and microheterogeneity of the biological environment (partially) control these processes.

Finally, we would like to argue that the quantitative modeling of the solute partitioning between water and 1-octanol will require the next generation of force fields that explicitly treat electrostatic polarization effects, because effective potentials, such as the TIP4P and OPLS models, are parametrized to reproduce the properties of neat liquids, thereby limiting the transferability of the potentials to other environments.

**Acknowledgment.** This paper is dedicated to Michael Klein on the occasion of his 60th birthday. We thank Pete Carr, Chris Cramer, and Don Truhlar for many stimulating discussions. Financial support from the National Science Foundation (CTS-9813601), a Sloan Research Fellowship, and a Doctoral Dissertation Fellowship (B.C.) is gratefully acknowledged. Part of the computer resources were provided by the Minnesota Supercomputing Institute.

JA001120+

---

(19) (a) Flynn, G. L. *J. Pharm. Sci.* **1971**, *60*, 345–353. (b) Smith, R. N.; Hansch, C.; Ames, M. M. *ibid.* **1975**, *64*, 599–606.

(20) Cabani, S.; Gianni, P.; Mollica, V.; Lepori, L. J. *Solution Chem.* **1981**, *10*, 563–595.